Complex Sphere Decoding with a Modified Tree Pruning and Successive Interference Cancellation

Li (Alex) Li, Rodrigo C. de Lamare, Alister G. Burr
Communications Research Group, Department of Electronics, The University of York, York, UK YO10 5DD
Email: ll550, rcdl500, agb1@ohm.york.ac.uk

***Abstract*—A novel complex sphere decoder is proposed in this paper, which achieves a lower complexity than existing techniques with the aid of successive interference cancellation (SIC), statistical pruning strategy (SPS) and a modified probabilistic tree pruning (MPTP) in the search strategy. In the proposed method, enumeration schemes can be avoided once the best partial path metrics (PPMs) fail to satisfy the constraint obtained by the MPTP for a given layer. In addition, the SIC provides a simple method to obtain the possible best candidate for each layer. This strategy effectively eliminates the extra branches without enumeration, if no candidates are available for each layer. Simulations illustrate that the proposed algorithm can reach near-maximum likelihood (ML) performance with a reduction in computational complexity.**

I. Introduction

Multi-input and multi-output (MIMO) architectures are a very promising technique for high data rate transmission. In order to achieve a high spectral efficiency, maximum likelihood (ML) detection should be employed with high order constellations. However, "brute-force" ML detection is impractical even for a small system. An alternative method is called the sphere decoder (SD), and this has attracted significant attention recently, due to the considerable complexity reduction it achieves [1], [2]. The key idea behind the SD is to find the lattice point closest to the received signals within the sphere radius. Although the computational complexity has been greatly reduced by Schnorr-Euchner enumeration (SE) [3], [4], sequential Fano decoders [5], and statistical pruning based algorithm [6]–[8], it is still very high for large numbers of antennas and high order constellations compared to suboptimal methods, such as linear or DFE based techniques [9], [10].

In most applications, the complex-valued system is decoupled and reformulated as an equivalent real-valued system. Real-valued SDs based on this approach can only process lattice based modulation schemes such as quadrature amplitude modulation (QAM) and pulse amplitude modulation (PAM), while other modulations such as phase shift keying (PSK) cannot be processed as efficiently, because some invalid lattice points are included in the search. Additionally, the depth of the expanded tree for real-valued SDs is twice that of complex counterparts. Hence, the complex-valued SE-SD and a modified version were proposed in [11], [12] respectively, which avoids the decoupling of the complex system and can be widely applied to other modulations without reaching invalid lattice points. Especially, the latter one has already achieved a very low complexity compared to other real-valued and complex-valued SDs [13]. However, the intricacy of complex SE enumeration is still a weak point that make the real-valued SDs preferred for hardware implementation. Besides the schemes described above, some novel low-complexity complex enumerators have been studied in [14]–[16], which are interchangeable in most complex-valued SDs. However, the enumeration still must be employed in each layer for several times. In the rest of this paper, the SDs we discuss are all based on complex-valued SE enumeration in [11], [12], namely computation of coordinate bound (CCB) enumeration.

Motivated by the description above and probabilistic tree pruning SD (PTP-SD) [7], we develop a novel complex-valued SD (CSD) with statistical pruning strategy (SPS), modified probabilistic tree pruning (MPTP) and SIC. There are three contributions in the proposed method: 1) The use of MPTP to reduce the number of nodes visited by evaluating the partial path metrics (PPMs) of the next layer's nulling-cancelling (NC) point. If the constraint of MPTP is not satisfied by the NC point (the best candidate) for a given layer, the complex SE enumeration can be avoided. (Note that other novel enumeration schemes can also be exploited to replace the CCB and sorting procedures in [11], [12] as stated above.) 2) For the SPS, the radius can be updated by the SPS at the bottom layer, if the first updated radius obtained by SIC is greater than the value given by SPS. This is done because if this is the case the radius updated by NC points is probably too large for the following search for some extreme cases. Compared to the proposed algorithm, the inter-search radius control scheme (ISRC) works in a similar way. But it must perform several Q-function and inverse Q-function calculations [8], and the parameters for ISRC are difficult to choose to maintain the tradeoff between complexity and performance. 3) Additional conditions for the CCB are specified by the proposed algorithm to avoid of missing possible candidates in each layer, which makes the candidates chosen by CCB more reliable with the reduced radius. Simulation results show that the proposed method can achieve a substantial complexity reduction as compared to existing CSD algorithms.

The rest of the paper is organized as follows. Section II presents the system model and problem formulation. Section III describes the conventional and proposed complex sphere decoder with relevant modifications as well as the algorithm table. In Section IV, the simulation results demonstrate the computational cost and bit error rate (BER) performance. The conclusions are drawn in Section V, and future directions for the work are indicated.

II. System Model

We consider the following complex-valued linear model:

$$\mathbf{r} = \mathbf{H}\mathbf{t} + \mathbf{v}, \tag{1}$$

where $\mathbf{r}$, $\mathbf{v} \in \mathbb{C}^{N_r}$, $\Re(\mathbf{t})(\Im(\mathbf{t})) \in \mathbb{R}^{N_t}$, $\mathbf{H} \in \mathbb{C}^{N_r \times N_t}$ has full column rank, and $\mathbb{R}$ and $\mathbb{Z}$ denotes the sets of complex numbers and real integers respectively. In wireless communications, $\mathbf{t}$, $\mathbf{r}$, and $\mathbf{v}$ are the transmit, receive, and the additive white Gaussian noise (AWGN) vectors.The latter follows the Gaussian distribution $\mathcal{CN}(\mathbf{0}_{N_r\times 1}, \sigma^2\mathbf{I}_{N_r\times 1})$. The quantity $\mathbf{H}$ is a random matrix that models the frequency-flat channel, the coefficients of which are i.i.d (independent and identically distributed) with complex Gaussian distribution. It randomly varies symbol by symbol. The channel state information is assumed to be known to the receiver perfectly. The ”brute-force” ML solution can be obtained by exhaustive search with exponentially increasing complexity. From the system model above, the ML solution can be expressed as

$$\widehat{\mathbf{t}}_{\text{ML}} = \underset{\mathbf{t}\in\mathcal{S}}{\operatorname{argmin}} \|\mathbf{r} - \mathbf{H}\mathbf{t}\|^2, \tag{2}$$

where $\mathcal{S}$ is the set of all possible transmit signal vectors with size $|\mathcal{S}| = M^{N_t}$. The quantity M denotes the constellation size for each transmit antenna.

III. The Proposed Complex Sphere Decoder

A. Review of the Conventional Complex Sphere Decoder

The channel matrix $\mathbf{H}$ in (2) can be decomposed into the matrices $\mathbf{Q}$ and $\mathbf{R}$ using a complex QR-decomposition given by

$$\mathbf{H} = \mathbf{Q}\mathbf{R} \quad \text{subject to} \quad \mathbf{Q}\mathbf{Q}^\dagger = \mathbf{I}_{N_r\times N_r}, \tag{3}$$

where $\mathbf{Q} \in \mathbb{C}^{N_r\times N_r}$ is an orthogonal matrix, $\mathbf{R} \in \mathbb{C}^{N_t\times N_t}$ is an upper triangular matrix whose diagonal elements are real values. It is noted that only the first N_t columns of $\mathbf{Q}$ and the first N_t rows of $\mathbf{R}$ are used, if $N_t \leq N_r$. The superscript $\dagger$ denotes the complex conjugate transpose. The tree structure system model can be described as

$$\mathbf{z} = \mathbf{Q}^\dagger\mathbf{r} = \mathbf{R}\mathbf{t} + \underbrace{\mathbf{Q}^\dagger\mathbf{v}}_{\mathbf{w}}. \tag{4}$$

The ML solution is given by

$$\begin{aligned}\widehat{\mathbf{t}}_{\text{ML}} &= \underset{\mathbf{t}\in\mathcal{S}}{\operatorname{argmin}} \|\mathbf{z} - \mathbf{R}\mathbf{t}\|^2 \\ &= \underset{\mathbf{t}\in\mathcal{S}}{\operatorname{argmin}} \sum_{i=1}^{N_t} \left| z_i - r_{i,i}t_i - \sum_{j=1}^{i-1} r_{i,j}t_j \right|^2,\end{aligned} \tag{5}$$

where $r_{i,j}$ denotes the $(N_t - i + 1, N_t - j + 1)$th element of $\mathbf{R}$, and z_i and w_i are the $(N_t - i + 1)$th entries of the vector $\mathbf{z}$ and $\mathbf{w}$, respectively.

1) Detection Ordering: The sorted QR decomposition (SQRD) is introduced to speed up the search in our algorithm [17], which can further consolidate the complexity reduction obtained by the proposed algorithm. Other advanced techniques can also be used such as MMSE-SQRD.

2) Computation of Coordinate Bound: This bound was first proposed in [11], and an improved version was presented in [12], which separates the constellation points into groups located on one or multiple concentric rings and computes the phase range based on the current sphere radius and previously detected symbols $\hat{t}_j$ and $r_{i,j}$. In this case, these constellation points can be tested according to the bound in Eq. (8) to determine whether they are in the circle of NC points. We assume $t_i^k = \gamma e^{i\theta_k}$, where t_i^k is the kth candidate constellation point at layer i, γ denotes the particular radius of one concentric ring of the constellation, and $0 \leq \theta_k < 2\pi$. The NC point for the ith layer can be defined as

$$\delta_i = \left(z_i - \sum_{j=1}^{i-1} r_{i,j}\hat{t}_j \right) \Big/ r_{i,i}, \tag{6}$$

and we thus calculate the phase range of θ_k as

$$\cos(\theta_k - \theta_{\delta_i}) = \frac{1}{2\gamma|\delta_i|}\left(\gamma^2 + |\delta_i|^2 - \frac{T_i}{r_{i,i}^2}\right) = \psi \tag{7}$$

where $T_i = T_0$. The candidates in layer i for a given concentric ring can be categorized as

$$\mathbf{t}_i^{\text{cand}} = \begin{cases} \emptyset, \psi > 1, \\ t_i^k, k = 1, 2, \ldots, M, \psi < -1 \\ t_i^k, \theta_k \in [\theta_{\delta_i} - \arccos(\psi), \theta_{\delta_i} + \arccos(\psi)], \\ -1 \leq \psi \leq 1, \end{cases} \tag{8}$$

where $0 \leq \arccos(\psi) \leq \pi$.

B. The Proposed Algorithm

We present a novel search strategy with the aid of SIC, and the MPTP algorithm to reduce the number of visited nodes and avoid the possible cost of the CCB, and SPS to control the updated radius and hence to further eliminate unnecessary candidates.

1) Search Strategy: Compared to conventional SE-CSD, the novel search strategy firstly performs SIC to obtain the NC points and the full path metric (FPM) without calculating the partial path metrics (PPMs) of other constellation points and sorting for each layer, and the radius T_0 may be updated by FPM or SPS T_s in III-B2 once the search reaches the bottom layer. The rest of the search can be performed upwards starting from the NC point of the bottom layer and not the top layer as in conventional SE-CSD. Additionally, the span of the search tree in Fig. **??** can be further shrunk by MPTP. In Eq. (7), the T_i can be replaced by ρ_i in III-B3 for CCB rather than T_0. Hence, the number of possible candidates for each layer can be significantly reduced. The details of the proposed algorithm are specified in Alg. 1.

2) Statistical Pruning Strategy: The possible radius for SDs can be calculated as $T_s = \sigma^2\beta$ according to [18].

$$\begin{aligned}\Pr(x < T_s) &= \int_0^{T_s/\sigma^2} \frac{1}{2^{N_t}(\sigma^2/2)^{N_t}} \frac{x^{N_t-1}}{\Gamma(N_t)} e^{-x/\sigma^2} dx \\ &= \int_0^{\beta} \frac{u^{N_t-1}}{\Gamma(N_t)} e^{-u} du \;, (x/\sigma^2 = u \,, \beta = T_s/\sigma^2) \\ &= 1 - \epsilon,\end{aligned} \tag{9}$$

where ϵ is the threshold probability defined according to the size of the system, the modulation and the number of possible ML solutions, the parameter β can be easily obtained by the inverse incomplete Gamma function. Once $T_0 > T_s$, the quantity T_0 will be replaced by T_s at the bottom layer.

3) Modified Probabilistic Tree Pruning: Denoting the detected symbols as $\hat{t}_j$, the noise w_i can be used to model the branch metric weight as

$$B_i = |z_i - \sum_{j=1}^{i} r_{i,j}\hat{t}_j|^2 \leq |w_i|^2, i = 1, 2, \ldots, N_t, \tag{10}$$

We assume the remaining $N_t - m$ layers' symbols are perfectly detected. Hence, the full metric weight can be represented as

$$P_m + \sum_{i=m+1}^{N_t} |w_i|^2 \leq T_0, \tag{11}$$

where $P_m = \sum_{i=1}^{m} B_i$. Since $\sum_{i=m+1}^{N_t} |w_i|^2/\sigma^2 \sim \chi^2$ with $2(N_t - m)$ degrees of freedom. The noise term can be given as $\sum_{i=m+1}^{N_t} |w_i|^2/\sigma^2 \leq (T_0 - P_m)/\sigma^2$. Accordingly, the probability of $\sum_{i=m+1}^{N_t} |w_i|^2/\sigma^2 \leq (T_0 - P_m)/\sigma^2$ is reasonably large, so that

$$\Xi((T_0 - P_m)/\sigma^2; N_t - m) = \epsilon_w < \epsilon_p, \tag{12}$$

where $\epsilon_w = \Pr(\sum_{i=m+1}^{N_t} |w_i|^2/\sigma^2 \leq (T_0 - P_m)/\sigma^2)$ and $\Xi(x; a) = \int_0^x \frac{1}{\Gamma(a)} e^{-t} t^{a-1} dt$. ϵ_p denotes the pre-defined probability of occurrence for the above event. According to (12), the PPM P_m becomes

$$P_m \leq T_0 - \sigma^2 \Xi^{-1}(\epsilon_p; N_t - m), \tag{13}$$

where $\Xi^{-1}(x; a)$ is the inverse of $\Xi(x; a)$. In other words, any PPM P_m larger than the LHS of (13) is unlikely to be the correct path for the ML solution, so these nodes with their child nodes are eliminated from the search tree. In order to avoid the CCB, we introduce the quantized NC point $Q(\delta_m)$ to calculate the best PPM for the mth layer as

$$B_m^{\delta} = \left| z_m - r_{m,m}Q(\delta_m) - \sum_{j=1}^{m-1} r_{i,j}\hat{t}_j \right|^2 + P_{m-1}, \tag{14}$$

and

$$B_m^{\delta} > \rho_m, \tag{15}$$

where $\rho_m = T_0 - \sigma^2 \Xi^{-1}(\epsilon_p; N_t - m)$, and $Q(\delta_m)$ is the constellation point obtained by CCB in Eq. (6) for the given mth layer. If the inequality in Eq. (15) is satisfied, the NC point and the remaining nodes with their child nodes are all pruned, and the CCB is not carried out, which saves the cost it introduces. Additionally, the quantity ρ_i is used in Eq. (7) to replace T_i to further reduce the number of candidates, and is pre-computed at the start of the transmission without any additional complexity.

C. Additional conditions for CCB

There are two additional conditions (AC) we should consider to avoid the performance loss, if we introduce $T_i = \rho_i$ as the intra radius for CCB.

1. If $\theta_{\delta_i} - \arccos(\psi) < 0$ and $\theta_{\delta_i} + \arccos(\psi) > 0$, set $-\pi \leq \theta_k < \pi$. If $0 \leq \theta_k < 2\pi$, some constellation points located in $[\pi, 2\pi]$ will be eliminated erroneously.
2. If $\theta_{\delta_i} + \arccos(\psi) > 2\pi$, set $\theta_{\delta_i} + \arccos(\psi) = \theta_{\delta_i} + \arccos(\psi) - 2\pi$. The upper limit of the phase range is greater than 2π that will cause the constellation points in $[0, \pi]$ will not be included.

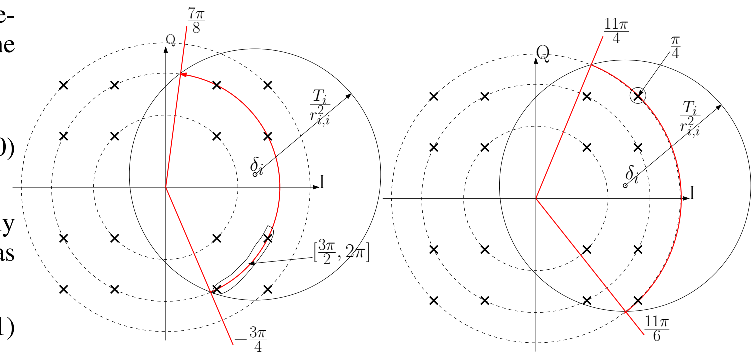

(a) Case I (b) Case II

Fig. 1: Additional conditions for two special cases

In Fig. 1, we present two special cases that can be fixed by the conditions described above. The phase range between $-\frac{3\pi}{4}$ and $\frac{7\pi}{8}$ is not matched to the above definition $0 \leq \theta_k < 2\pi$, so the two points between $\frac{3\pi}{2}$ and 2π will be pruned erroneously in Fig. 1a within the red circle. For Fig. 1b, the phase of the constellation point is $\frac{\pi}{4}$, which should be considered as a candidate based on the phase range. But the upper limit of phase range obtained by CCB is greater than 2π, which will eliminate the candidate at $\frac{\pi}{4}$. Note that these additional conditions are not specified in previous works such as [11], [12]. For PSK modulation and 4QAM, all constellation points are located on one ring, and the candidates can be obtained in one shot. For high order QAM, the CCB must be performed for different concentric rings.

Algorithm 1 Proposed complex sphere decoder

Input: $T_0 = \infty$, $\mathbf{R}$, $\mathbf{z}$, $\rho_i, i = 1, 2, \ldots, N_t$.
Output: $\widehat{\mathbf{t}}_{\text{ML}}$

1: Compute the NC points and obtain the full path metric and partial path metrics $P^1_{1,\ldots,N_t}$, save $t_{1,\ldots,N_t}$, $\widehat{\mathbf{t}}_{\text{ML}} = \widehat{\mathbf{t}}$.
2: **If** $T_s < P_{N_t}$, $P_{N_t} = T_s$. **end**. Set $T_0 = P_{N_t}$. Perform step 6, and set $k_i = 1, \forall i$.
3: Set $i = N_t$, go to 17.
4: Compute the PPM B_i^{δ} according to (6) and (14).
5: **If** $B_i^{\delta} > \rho_i$, go to 17.
6: **Else** obtain the sorted candidates $t_i^{k_i} \in \mathbf{t}_i^{\text{cand}}, k_i = [1, 2, \ldots, N_c^i]$ in (8) by the complex SE enumeration (CCB) with ρ_i.
Set $k_i = 0$.
7: **end**
8: $k_i = k_i + 1$.
9: **If** $k_i \leq N_c^i$ or $i = N_t$, go to 12.
10: **Else** go to 17.
11: **end**
12: Calculate the PPM for the kth candidate at the ith layer, $P_i^{k_i} = B_i^{k_i} + P_{i-1}$.
13: **If** $i = N_t$, $P_{N_t} = P_i^{k_i}$, go to 20. **end**
14: **Else** go to 16.
15: **end**
16: **If** $P_i^{k_i} < T_0$, $i = i + 1, P_{i-1} = P_{i-1}^{k_{i-1}}$, save t_{i-1}, go to 4. **end**
17: $i = i - 1$.
18: **If** $i = 0$, output $\widehat{\mathbf{t}}_{\text{ML}}$ and terminate.
19: **Else** go to 8.
20: **end**
21: **If** $P_{N_t} < T_0$. $T_0 = P_{N_t}$,
22: **If** $T_s < T_0$, $T_0 = T_s$. **end**
23: $\widehat{\mathbf{t}}_{\text{ML}} = \widehat{\mathbf{t}}$, go to 17.
24: **end**

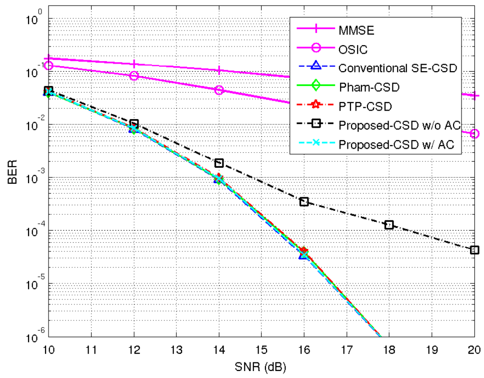

(a) BER

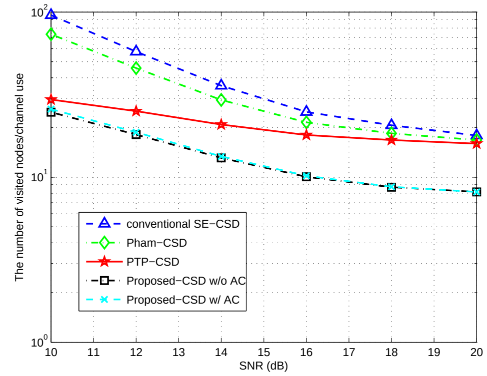

(b) Visited nodes

Fig. 2: Comparison of BER and then number of visited nodes per channel use with perfect channel estimates between the proposed and other CSDs for $N_t = N_r = 8$ with 16QAM. red Note that the curves of Conventional SE-CSD, Pham-CSD, PTP-CSD and proposed-CSD w/ AC are superimposed in (a).

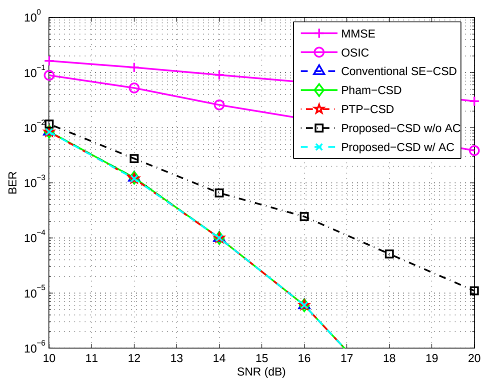

(a) BER

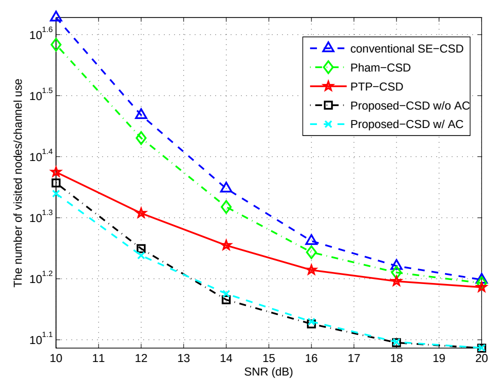

(b) Visited nodes

Fig. 3: Comparison of BER and the number of visited nodes per channel use with perfect channel estimates between the proposed and other CSDs for $N_t = N_r = 8$ with 8PSK. Note that the curves of Conventional SE-CSD, Pham-CSD, PTP-CSD and proposed-CSD w/ AC are superimposed in (a).

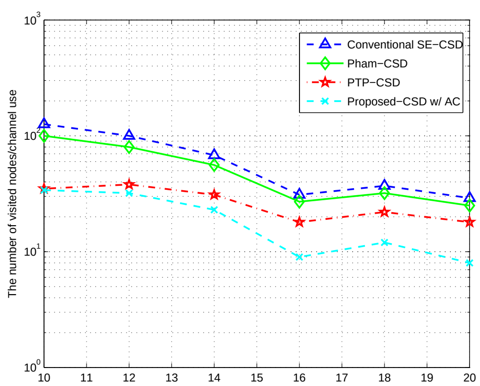

Fig. 4: Worst case complexity of CSDs against SNR, $N_t = N_r = 8$ with 16QAM

IV. Simulation Results

In this section, the performance and complexity of several CSDs are compared in terms of bit error rate (BER) and the number of visited nodes in a 8×8-MIMO system with 16QAM and 8PSK. An MPSK modulation in our simulation is defined as $\gamma e^{(2n+1)\pi/M} : n = 0, 1, \ldots, M-1$. We consider the conventional SE-CSD, Pham-CSD [12], PTP-CSD [7], the proposed CSD with and without additional conditions for CCB, all of which are complex SE enumeration based CSD with $T_0 = \infty$ at the beginning of the search. The PTP can be simply extended to Pham-CSD. The signal-to-noise ratio (SNR) is defined as $\text{SNR(dB)} = 10\log_{10}\left(\frac{E_s N_r}{\sigma^2}\right)$. The probabilistic noise constraint is set to $\epsilon_p = 0.2$. The threshold ϵ for SPS must be appropriately adjusted according to the dimensions and the modulation as stated earlier, and we set $\epsilon = 0.001$. The ISRC scheme [8] is not employed, because of the difficulty of choosing parameters. As shown in Figs. 2 and 3, the complexity of the proposed CSD improves upon the others in terms of visited nodes per channel use by over 25% for 16QAM and more than 25% for 8PSK at high SNRs without any BER performance loss, even compared to conventional SE-CSD in the mid and high SNR regime. The performance loss of the proposed algorithm without additional conditions (AC) is significant at high SNRs. In other words, it is more sensitive to the missing candidates in low noise scenarios. However, the complexity reduction is not obvious at low SNR scenarios due to the CCB including more unreliable constellation points. It is well known that the complexity of SDs will converge at very high SNR values, so the improvement of the proposed SD is reduced at high SNR, but is still very promising. The worst case complexity (the number of visited nodes is greater than the numbers of 99% of channel uses' visited nodes) of CSDs are also plotted in Fig. 4, which implies that the number of visited nodes of the proposed

CSD is tightly lower bounded by the complexity of SIC at high SNRs. Additionally, the complexity of SDs increases exponentially with increasing dimension. We therefore plot the number of visited nodes against the dimensions ($N_t = N_r$) at a high SNR value (20dB) to show that the complexity is still reduced by our proposed algorithm in Fig. 5. The complexity discussed so far is only based on the number of visited nodes. In order to show the advantages of avoiding complex SE enumeration (CCB) and eliminating unnecessary candidates, the curves with the number of FLOPS are presented in Fig. 6. The proposed algorithm still outperforms the other CSDs, because of fewer implementations of complex SE enumeration and the reduced number of candidates. The number of FLOPS of detection ordering are not considered, because the CSDs are performed with the same preprocessing technique. Furthermore, the parameters for MPTP can be pre-computed before the start of the transmission.

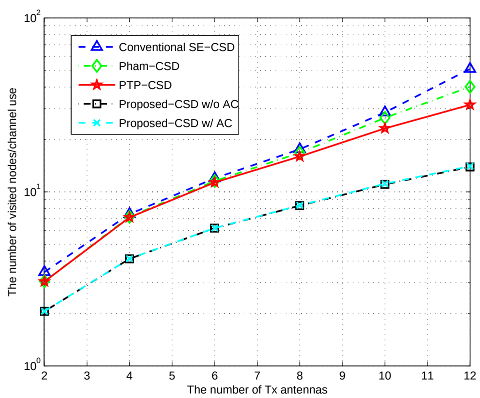

Fig. 5: The number of visited nodes against increasing dimensions $N_t = N_r$

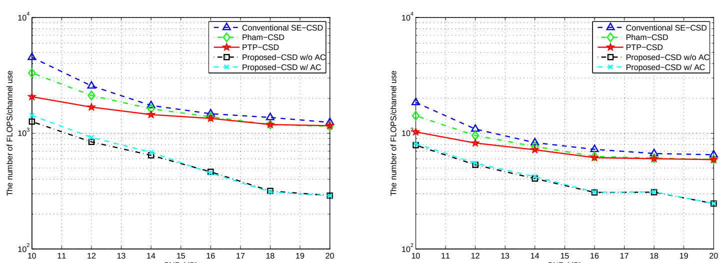

(a) 16QAM (b) 8PSK

Fig. 6: Comparison of FLOPS between the proposed and other CSDs for $N_t = N_r = 8$ with 16QAM and 8PSK

V. Conclusion

In this paper, we have presented a novel complex-valued SD to further reduce the complexity by employing MPTP, SPS and SIC, which can specify a probabilistic noise constraint to control the CCB and the number of visited nodes with the aid of SPS and SIC. The future direction of the proposed method can be naturally extended to list SD (LSD) [11] to reduce the computational cost for the maximum a posteriori (MAP) detector.

References

[1] E. Viterbo and J. Boutros, “A universal lattice code decoder for fading channels,” *IEEE Trans. Inf. Theory*, vol. 45, no. 1639-1642, p. 45, Jul. 1999.

[2] M. O. Damen, H. E. Gamal, and G. Caire, “On maximum-likelihood detection and the search for the closest lattice point,” *IEEE Trans. Inf. Theory*, vol. 49, pp. 2389–2402, Oct. 2003.

[3] C. P. Schnorr and M. Euchner, “Lattice basis reduction: Improved practical algorithms and solving subset sum problems,” *Math. Program.*, vol. 66, pp. 181–191, 1994.

[4] E. Agrell, T. Eriksson, A. Vardy, and K. Zegar, “Closet point search in lattices,” *IEEE Trans. Inf. Theory*, vol. 48, pp. 2201–2214, Aug. 2002.

[5] A. D. Murugan, H. E. Gamal, M. O. Damen, and G. Caire, “A unified framework for tree search decoding: rediscovering the sequential decoder,” *IEEE Trans. Inf. Theory*, vol. 52, no. 3, pp. 933–953, Mar. 2006.

[6] R. Gowaikar and B. Hassibi, “Statistical pruning for near-Maximum likelihood decoding,” *IEEE Trans. Signal Process.*, vol. 55, pp. 2661–2675, Jan 2007.

[7] B. Shim and I. Kang, “Sphere decoding with a probabilistic tree pruning,” *IEEE Trans. Signal Process.*, vol. 56, pp. 4867–4878, Oct. 2008.

[8] ——, “On further reduction of complexity in tree pruning based sphere search,” *IEEE Trans. Commun.*, vol. 58, no. 2, pp. 417–422, Feb. 2010.

[9] G. J. Foschini, “Layer space-time architecture for wireless communication in a fading environment when using multiple antennas,” *Bell Labs Tech. Journal*, vol. 1, no. 2, pp. 41–59, 1996.

[10] R. C. de Lamare and R. Sampaio-Neto, “Minimum mean squared error iterative successive parallel arbitrated decision feedback detectors for DS-CDMA systems,” *IEEE Trans. Commun.*, vol. 56, no. 5, pp. 778–789, May 2008.

[11] B. Hochwald and S. ten Brink, “Achieving near-capacity on a multiple-antenna channel,” *IEEE Trans. Commun.*, vol. 51, pp. 389–399, Mar. 2003.

[12] D. Pham, K. R. Pattipati, P. K. Willett, and J. Luo, “An improved complex sphere decoder for V-BLAST systems,” *IEEE Signal Process. Lett.*, vol. 11, pp. 748–751, Sep. 2004.

[13] K.-C. Lai and L.-W. Lin, “Low-complexity adaptive tree search algorithm for MIMO detection,” *IEEE Trans. Wireless Commun.*, vol. 8, no. 7, pp. 3716–3726, Jul. 2009.

[14] A. Burg, M. Borgmann, M. Wenk, M. Zellweger, W. Fichtner, and H. Bölcskei, “VLSI implementation of mimo detection using the sphere decoding algorithm,” *IEEE Journal of Solid State Circuits*, vol. 40, pp. 1566–1577, 2005.

[15] M. Shabany, K. Su, and P. Gulak, “A pipelined scalable high throughput implementation of a neak-ML K-Best complex lattice decoder,” in *in Proceedings IEEE ICASSP*, 2008, pp. 3173–3176.

[16] M. Barrenechea, M. Mendicute, I. Jimenez, and E. Arruti, “Implementation of complx enumeration for multiuser MIMO vector precoding,” in *19th European Signal Processing Conference (EUSIPCO 2011)*, Barcelona, Spain, Sep. 2011, pp. 739–743.

[17] D. Wübben, J. Rinas, R. Böhnke, V. Kühn, and K. D. Kammeyer, “Efficient algorithm for detecting layered space-time codes,” in *Proc. ITG Conference on Source and Channel Coding*, Berlin, Germany, Jan. 2002.

[18] B. Hassibi and H. Vikalo, “On the sphere-decoding algorithm I. Expected complexity,” *IEEE Trans. Signal Process.*, vol. 53, pp. 2806–2818, Aug. 2005.